Analysis of the seismic origin of landslides: Examples from the New Madrid seismic zone

RANDALL W. JIBSON   U.S. Geological Survey, Box 25046, M.S. 966, Denver Federal Center, Denver, Colorado 80225
DAVID K. KEEFER   U.S. Geological Survey, 345 Middlefield Road, M.S. 998, Menlo Park, California 94025

ABSTRACT

By analyzing two landslides in the New Madrid seismic zone, we develop an approach for judging if a landslide or group of landslides of unknown origin was more likely to have formed as a result of earthquake shaking or in aseismic conditions. The two landslides analyzed are representative of two groups of landslides that previous research on the geomorphology and regional distribution of landslides in this region indicates may have been triggered by the 1811–1812 New Madrid earthquakes. Slope-stability models of aseismic conditions show that neither landslide is likely to have formed aseismically even in unrealistically high ground-water conditions. Dynamic stability analysis using Newmark's method shows that both slides probably would have experienced large inertial displacements during earthquake shaking similar to that which occurred in 1811–1812; these displacements are large enough that catastrophic failure is highly probable. Thus, the stability analyses are consistent with other lines of evidence that these landslides formed as a result of strong earthquake shaking during the 1811–1812 earthquakes.

Our analysis yields a general relationship between Newmark landslide displacement, earthquake shaking intensity, and the critical acceleration of a landslide. Using this relationship, we estimate the minimum shaking intensities required to trigger the types of landslides studied: an $m_b = 5.8$ or M = 5.9 earthquake is the lower bound threshold at zero epicentral distance that could trigger catastrophic movement of typical block slides in the New Madrid seismic zone; for earth flows, $m_b = 5.4$ or M = 5.3 is the threshold earthquake.

INTRODUCTION

Among the most dramatic effects of the New Madrid earthquakes of 1811–1812 were the numerous landslides along the bluffs bordering the Mississippi alluvial plain in western Tennessee and Kentucky (Fuller, 1912).

Many landslide features are currently visible along the bluffs in the epicentral area of the 1811–1812 earthquakes, but determining which, if any, of these features were triggered in 1811–1812 is a complex and difficult problem. In this paper, we address a single fundamental question: can a landslide of unknown origin be analyzed to assess the relative likelihood of failure in seismic versus aseismic conditions?

In recent studies (Jibson and Keefer, 1988, 1989), described in more detail below, we analyzed field and historical data and the regional distribution of landslides in the epicentral area. The data and conclusions from these studies, which were based on a consideration of the entire group of landslides at a regional scale, indicate that many of these landslides probably were triggered by the 1811–1812 earthquakes. In the present paper, we use static and dynamic slope stability analyses to show that two representative landslides in the epicentral area are much more likely to have been triggered by strong earthquake shaking, similar to that generated in 1811–1812, than by changes in ground-water levels in aseismic conditions. A detailed analysis of the stability of these individual landslides provides a firmer basis for our interpretation of the ground-failure effects of the 1811–1812 earthquakes and will help us to predict the conditions necessary to trigger widespread landsliding in future earthquakes in the New Madrid seismic zone.

The successful application of the approach detailed in this paper also establishes a procedure for judging the probable cause of failure of landslides elsewhere. The ability to assess the likelihood of a landslide having formed as a result of earthquake shaking as opposed to other factors opens several opportunities for using landslide analysis to interpret the recent geologic record. For example, dating landslides that are likely to have formed during earthquake shaking would be valuable in paleoseismic studies, particularly in areas such as the central United States where exposures of seismogenic faults are rare or absent.

In this paper, we review the geological and seismological context of the study, present the geotechnical data needed for analysis of the stability of two representative landslides, and interpret the origin of these landslides in light of the results of the analyses. Further, we document a more general procedure for determining the likelihood that old landslides were triggered by earthquakes and propose a general quantitative relationship between earthquake shaking intensity and seismic slope stability that is applicable to seismic hazard analysis.

GEOLOGIC SETTING

The area affected by major landsliding triggered by the 1811–1812 earthquakes encompasses more than 300 km of bluffs that form the eastern edge of the Mississippi alluvial plain between Cairo, Illinois, and Memphis, Tennessee (Fig. 1). The bluffs lie along the eastern flank of the northern Mississippi embayment, a broad, south-southwest–plunging syncline, the axis of which approximately coincides with the Mississippi River. Embayment deposits exposed in the bluffs generally dip to the west-northwest in most of the area.

These ancestral bluffs generally are separated from the Mississippi River by a broad alluvial plain; thus, they are subject to landsliding from fluvial erosion in only a few locations. The bluffs stand as high as 70 m above the alluvial plain of the Mississippi River and therefore are not subject to landsliding from conditions such as rapid drawdown because the bluff is never inundated to a significant height by flooding. Average bluff height is 35 m; slope angles, ranging from a few degrees to almost vertical, generally are 15°–25°.

The Eocene Jackson Formation (Conrad, 1856) forms the base of the bluffs throughout most of the area. Exposures are as thick as 45 m in the lower part of the bluffs. The com-
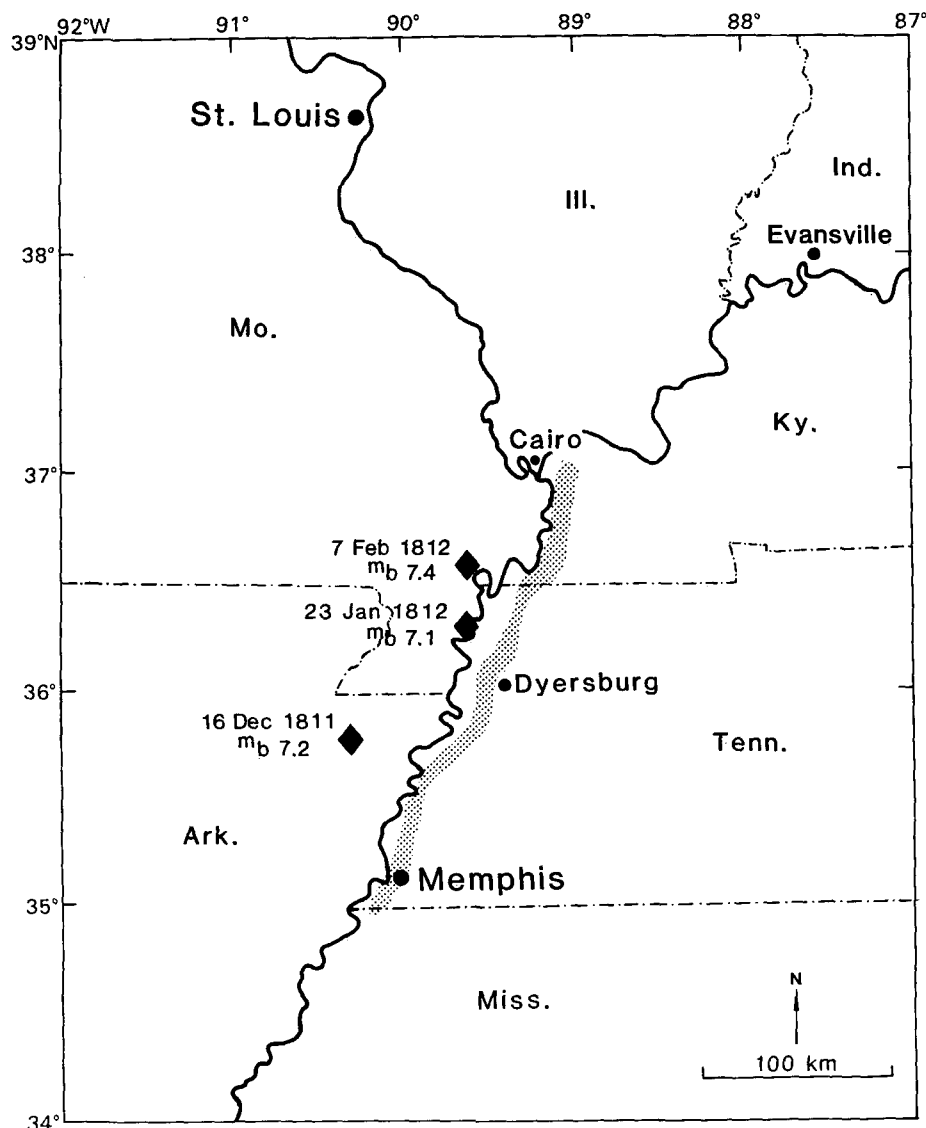
Figure 1. Study area (shaded) and estimated epicenters (diamonds), dates, and estimated body-wave magnitudes of the three largest earthquakes in the 1811–1812 sequence (earthquake locations and magnitudes from Nuttli, 1983).

quence, the most severe seismic event in historical times in the central and eastern United States. The three largest events, which occurred on 16 December 1811, 23 January 1812, and 7 February 1812, had estimated magnitudes corresponding to 7.1–7.4 on the body-wave magnitude (m_b) scale (Nuttli, 1973) and 8.1–8.3 on the moment magnitude (M) scale (Hamilton and Johnston, 1990). Thousands of aftershocks shook the area for many months, several of which were at least of moderate intensity (Nuttli, 1973).
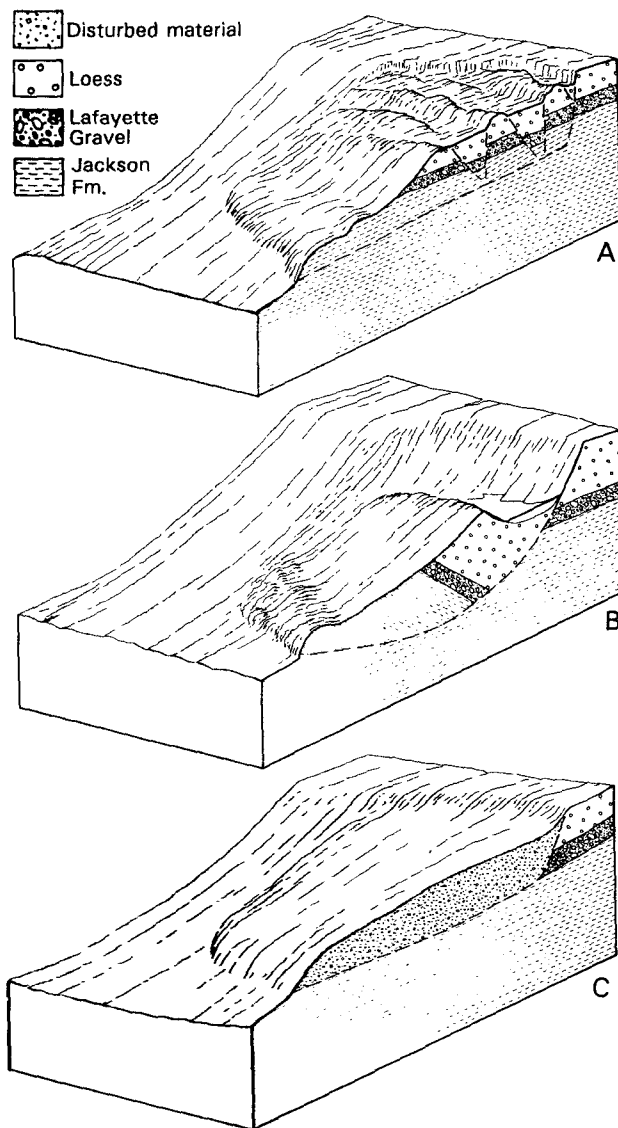
The effects of the 1811–1812 earthquake sequence have been described by Fuller (1912) and Nuttli (1973); liquefaction effects were further documented by Saucier (1977) and Obermeier (1989). The epicentral area of greatest damage included ~130,000 km² (Fuller, 1912). Within this region, uplift and subsidence of as much as a few meters occurred over hundreds of square kilometers, the most notable area of subsidence being Reelfoot Lake in northwestern Tennessee. Fissuring of the ground surface and caving of river banks also was widespread, and more than 650 km² of timber was destroyed by flooding, violent ground shaking, or landsliding (Fuller, 1912). Liquefaction of subsurface sand layers inundated ~10,000 km² with as much as 2 m of sand and water. Not surprisingly, eyewitness accounts describe the entire land surface as being disrupted and, in many places, uninhabitable (Penick, 1981). Pertinent to this study are reports of landslides along the bluffs in western Tennessee and Kentucky from Hickman, Kentucky, at least to the Obion River, near Dyersburg, Tennessee (Fuller, 1912).

The New Madrid seismic zone has produced 20 damaging earthquakes since 1811–1812 (Nuttli, 1982), and it continues to be the most active seismic zone east of the Rocky Mountains (Hamilton and Johnston, 1990).

position of the Jackson Formation is highly variable, but it generally consists of discontinuous layers of shallow-marine embayment deposits of clay and silt, ranging from a few centimeters to several meters thick. The Eocene beds generally dip a few degrees west-northwest (out of the bluff face in most of the area), but the amount and direction of dip vary locally; the amount of dip is generally less than 20°.

As much as 20 m of Pliocene terrace gravel and sand of the Lafayette Gravel lies unconformably on the Jackson Formation (McGee, 1891; Potter, 1955). The gravel and sand lenses are commonly uncemented but at some localities contain concretionary beds as

thick as 2 m. The Lafayette Gravel is saturated locally where water tables are perched, and it probably is subject to large seasonal fluctuations in ground-water conditions. The unit pinches out in some areas.

The bluffs are capped by 5–50 m of Pleistocene loess lying unconformably on the Lafayette Gravel and Jackson Formation. The average thickness of the loess is about 15 m. Loess is glacially derived, eolian silt that commonly forms nearly vertical faces.

SEISMIC HISTORY

The bluffs are in the epicentral region of the 1811–1812 New Madrid earthquake se-

DESCRIPTION OF LANDSLIDES IN THE AREA

Along the bluffs in the study area, 221 large (greater than 60-m-wide) landslides were identified on air photos, examined on the ground, classified morphologically (after Varnes, 1978), and plotted on an inventory map (Jibson and Keefer, 1988). Three classes of landslides were mapped: old coherent slides, earth flows, and young rotational slumps.

Old coherent slides (Fig. 2) constitute 65% of the landslides in the study area. This group includes translational (block) slides and rotational slides (slumps), both of which remained

Figure 2. Idealized drawings of types of landslides along the bluffs. These landslides all have eroded, revegetated features; no active analogues are present in the area. A. Old coherent translational block slide. B. Old coherent rotational slump. C. Earth flow.

present only along bluffs where the Mississippi River has impinged since 1820 (about 11% of bluff length); because of this recent fluvial erosion, bluffs in these reaches are much steeper than bluffs away from the river where old coherent slides and earth flows are present. The young slumps are characterized by massive single slump blocks that form where the river has undercut the bluffs. They are differentiated from old slumps based on less rotation, less scarp and head erosion, absence of multiple blocks, and, in some cases, absent or young vegetation (Jibson and Keefer, 1988).

PREVIOUS WORK

The two earliest field investigations of the landslides, conducted in 1891 (McGee, 1893) and 1904 (Fuller, 1912), suggest that at least some of the old coherent slides in part of the area formed during the 1811–1812 earthquakes. More recent studies (Jibson and Keefer, 1984, 1988; Jibson, 1985) used dendrochronology, geomorphology, historical topographic maps, local historical accounts, and comparisons with landslides triggered by other earthquakes to show that the apparent ages and morphologies of most of the old coherent slides and earth flows are consistent with triggering during the 1811–1812 earthquakes. The evidence further shows that the only ongoing, large, aseismic landslide activity in the area results from fluvial undercutting of near-river bluffs, which triggers slumps that are morphologically distinct from the old coherent slides on bluffs away from the river. The landslides on bluffs away from the river all appear to be about the same age, which suggests a common triggering event; these landslides are unrelated to fluvial activity and have no active analogues in the area (Jibson and Keefer, 1988).

In a statistical analysis of the regional distribution of the three types of landslides along the bluffs, we (Jibson and Keefer, 1989) used discriminant analysis and multivariate linear regression to measure correlation between landslide distribution and slope height and steepness, stratigraphic variation, slope aspect, and proximity to the hypocenters of the 1811–1812 New Madrid earthquakes. The discriminant analysis shows no spatial correlation between young rotational slumps and the earthquakes. Bluffs having old coherent slides and earth flows, however, are significantly closer to the estimated hypocenters of the 1811–1812 earthquakes than are bluffs without these slides (Jibson and Keefer, 1989). Multiple regression analysis, which si-

fairly intact or coherent. These slides are termed "old" because they all are eroded and revegetated and show no sign of activity for at least the past several decades. They all appear to be of similar age based primarily on amount of scarp retreat, degree of erosion of ridges, and vegetation density and age on scarps and disrupted areas (Jibson and Keefer, 1988). These landslides are deep seated (typically deeper than 20 m) and have basal shear surfaces in the clayey Jackson Formation that forms the base of the bluffs. The translational block slides (Fig. 2 A) are characterized by horst and graben topography, and toe areas commonly have compressional ridges in front of the landslide blocks that moved down and out (as far as 100 m) from the parent slope. Basal shear surfaces dip 4°–25°. The old rotational slumps (Fig. 2 B) are characterized by

either single or multiple blocks that appear to have rotated a large amount relative to the younger slumps described subsequently.

Earth flows (Fig. 2C) constitute 24% of the landslides. Characteristic features are gently hummocky topography and ridges of accumulated material in the toe area. A few deforested earth-flow complexes contain recently (0–5 yr) active flows. The large majority of the earth flows, however, including all those on forested slopes, are eroded and revegetated and have been inactive for at least the past several decades. As with the old coherent slides, the degree of erosion and revegetation suggests similar ages for the earth flows (Jibson and Keefer, 1988).

The remaining 11% of the landslides are young rotational slumps. Young slumps are
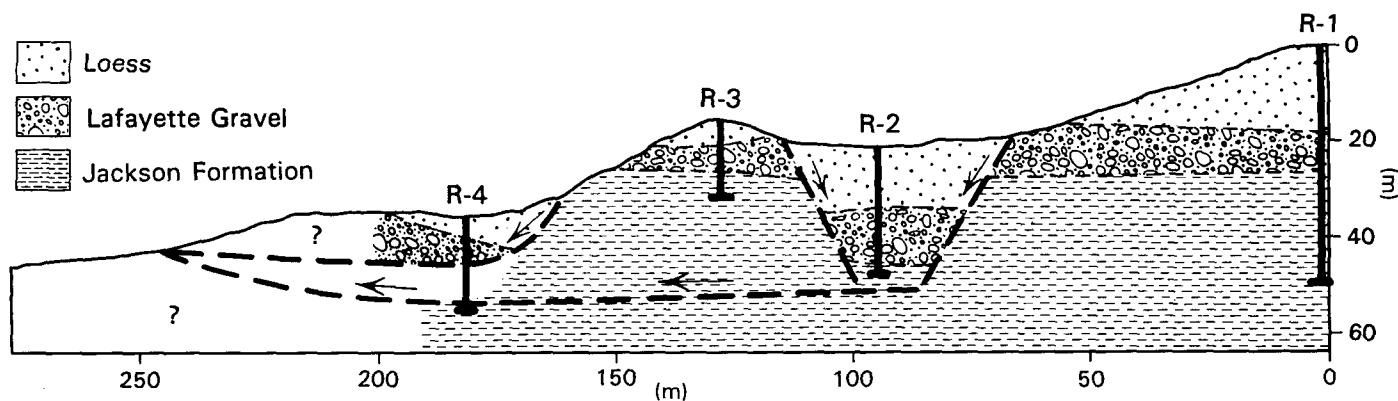
Figure 3. Profile of Stewart landslide showing subsurface stratigraphy (from drill holes located in Fig. 4) and diagrammatic representation of failure surfaces (dashed lines). Intact stratigraphy is shown at R-1.

multaneously combined all factors, likewise indicates no correlation between the distribution of young rotational slumps and the earthquake locations. The distribution of the old coherent slides and earth flows, however, strongly correlates with proximity to the hypocenters of the 1811–1812 earthquakes, as well as with slope height and aspect (Jibson and Keefer, 1989). The results of these statistical analyses thus show that the old coherent slides and earth flows in the area are spatially related to the 1811–1812 earthquake hypocenters.

The methods and conclusions from these previous studies do not address the questions of whether any specific landslide in the area was actually triggered in 1811–1812 or what conditions likely led to the failure of a given landslide. The following sections describe an approach to address these questions.

ANALYSIS OF THE STEWART AND CAMPBELL LANDSLIDES

We chose two landslides for detailed analysis: the Stewart landslide, a translational block slide 11 km north of Dyersburg, Tennessee; and the Campbell landslide, an earth flow 10 km west of Dyersburg (Fig. 1). These slides represent the two types of old landslides in the area that previous research indicates may have been triggered by the 1811–1812 earthquakes.

Description of Stewart Landslide

The Stewart landslide averages 800 m wide by 400 m long and covers ~0.3 km². Large parts of the slide are heavily forested, which precluded detailed topographic mapping. Figure 3 shows a profile of the Stewart slide; subsurface data are from drilling along the line of profile.

The broad, bowl-shaped scarp forms a re-entrant in the local bluff line; below the scarp, several large horst and graben blocks from prominent but discontinuous ridges and troughs that interfinger with one another and create a complex topography. The grabens commonly have sloping bottoms that allow drainage; however, one ephemeral sag pond is in a closed depression on a graben block.

Most of the landslide blocks did not rotate and apparently translated with little internal deformation on a gently sloping basal shear surface. The horst block shown on the profile (Fig. 3) is displaced downward only 3 m but moved horizontally about 50 m. Thus, the basal shear surface dips less than 4°. Below the main landslide blocks, there is a hummocky toe area formed from subsidiary slumping from the displaced bluff face (Fig. 3) and compression of the material at the base of the slope.

Description of Campbell Landslide

The Campbell landslide is a large complex of coalescing earth flows that extends almost 4 km along the bluffs. Dense tree cover made detailed mapping infeasible; a profile is shown in Figure 4. Individual earth flows in the complex average about 400 m long, and the complex covers about 1.5 km².

The Campbell slide has subtle features: gently hummocky slopes of 5°–10° lie downslope from a 20° scarp near the top of the bluff. Discrete lobes and an irregular scarp visible
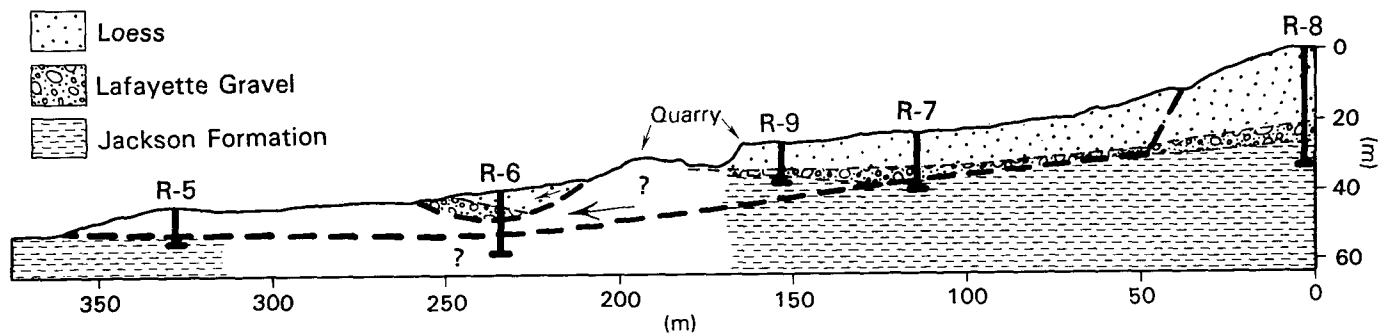

Figure 4. Profile of Campbell landslide showing subsurface stratigraphy (from drill holes located in Fig. 6) and diagrammatic representation of failure surfaces (dashed lines). Intact stratigraphy is shown at R-8.

on air photos indicate that landsliding initiated at several localities and coalesced to form a continuous complex. All of these lobes appear to be the same age; evidence of recent movement (such as tilted trees, ground cracks, or young scarps) is absent except in deforested areas where smaller active earth flows are present (Jibson and Keefer, 1988). A gentle compressional ridge extends along the base of the bluff where material moved downslope to an area flat enough to inhibit movement and cause accumulation (Fig. 4). The break in slope in the profile (Fig. 4) between the toe and the head scarp is probably a secondary scarp. The location of the disturbed zone in the drill holes (Fig. 4) and the surface morphology of the slide indicate that sliding probably occurred along a shear surface that dips subparallel to the ground surface at about 5° from the horizontal.

Premise of the Analyses

The intent of the analyses of these representative landslides was to estimate the probable conditions leading to failure. We therefore analyzed both slides in static (aseismic) conditions to determine the likelihood of failure caused by changes in ground-water conditions in the absence of earthquake shaking. We then analyzed both slides in dynamic (seismic) conditions to judge if failure would have occurred in earthquake shaking similar to that produced in 1811–1812. Analytical results showing (1) that the bluffs are very stable in aseismic conditions even in the worst conceivable ground-water conditions and (2) that the bluffs probably would fail catastrophically in severe earthquake shaking, would provide strong evidence, consistent with other lines of evidence (Jibson and Keefer, 1988; 1989), that these landslides did, indeed, form as a result of the 1811–1812 earthquakes.

For this approach to be valid, two assumptions must be reasonably satisfied: (1) the properties (geometry, shear strength, and so forth) of the slope at present are the same as those at the time the landslide formed, and (2) these properties can be accurately characterized.

The first assumption is reasonable because the unfailed bluffs adjacent to our landslides appear geomorphically stable at a time scale of several decades to a few centuries; they are stable with respect to surface erosion and deep-seated mass movement and are not subject to fluvial erosion that would alter their morphology. They support dense, undisturbed vegetation and have simple, stable slope profiles. Thus, we can fairly confidently reconstruct the prelandslide bluff morphol-

ogy. Further, the slip surfaces of both landslides extend primarily through the Eocene deposits and secondarily through Pliocene and Pleistocene deposits. Significant changes over decades to centuries in the geometry or geotechnical properties of deposits several thousands to several tens of millions of years old are extremely unlikely, and we know of no processes acting in this area that could precipitate such rapid change. Therefore, the first assumption is reasonably supported.

The second assumption—that the slope properties can be characterized accurately—is more subjective. How accurate is accurate enough? The morphology of the slope is simple and stable and can be characterized easily. The stratigraphy and geotechnical properties of the slope materials can be characterized only by a subsurface investigation, which requires sampling, geotechnical testing, interpretation, and interpolation. The geotechnical investigation described below is one of the most extensive ever carried out for such a study, and the results produced a reasonable and consistent characterization of the sites. The conclusions from such an idealization of actual conditions must be interpreted in the context of the inherent uncertainty present in any such investigation.

Geotechnical Investigation

The purpose of the geotechnical investigation was to procure soil samples and conduct laboratory and *in situ* engineering tests to determine the soil properties that affect slope stability. Fundamental properties required for stability analyses are soil unit weight and shear strength. Index properties such as grain size, plasticity, water content, and color are determined to classify the soils and correlate soil layers between sample sites.

We drilled nine rotary boreholes on the two landslides from which we procured split-spoon samples from Standard-Penetration Testing (SPT) and 13-cm-diameter undisturbed piston cores. Split-spoon samples are obtained by hammering a steel sampler into the bottom of the borehole; the types of materials in our study area typically are heavily disturbed by this process, and such samples are used primarily for determining index properties. Piston cores are procured by carefully pushing a thin-walled steel tube into the bottom of the borehole; piston cores provide nearly undisturbed soil samples that are used to measure soil unit weight and shear strength. Additional samples were carved from surface outcrops and obtained by hand augering; these samples were used primarily

to determine index properties, but some block samples were of sufficient quality to allow shear-strength testing. A detailed description of the sampling techniques used is given by Jibson (1985).

Soil shear strength commonly is characterized in one of two ways, depending on the conditions being considered (Newmark, 1965; Lambe and Whitman, 1969). In static (aseismic) conditions, drained or effective shear strength is characterized using two components: the angle of internal friction (ϕ') and the cohesion (c'). The pore-water pressure is assumed to be measurable or estimable and is accounted for explicitly in the stability analysis, and no pore-water pressures in excess of hydrostatic are present. In dynamic (seismic) conditions, undrained or total shear-strength parameters are used. During earthquakes, slope materials behave in an undrained manner because excess pore-water pressures induced by dynamic deformation of the soil column cannot dissipate during the relatively brief duration of the shaking. Undrained strength also is called "total strength" because the respective contributions of friction, cohesion, and pore pressure are not differentiated, and the total strength is expressed as a single quantity.

Drained shear strengths of undisturbed soil samples were measured by direct shear and consolidated-undrained (CUTX) triaxial shear (Jibson, 1985). Direct shear tests were run slowly enough to allow full drainage (no excess pore pressure), and the frictional and cohesive components of the shear strength were measured directly under different normal loads. Direct-shear samples were sheared parallel to bedding, which approximates the geometry of the basal shear surface. In triaxial tests, no drainage is allowed, but pore pressures are measured throughout the test and can be mathematically removed from the results to estimate drained conditions. Failure is induced at an angle oblique to bedding; thus, CUTX friction angles tend to be slightly greater than those measured in direct shear.

Undrained shear strengths were measured primarily by CUTX tests. CUTX results were supplemented by vane shear, penetrometer, and correlation with SPT blow counts where undisturbed samples were unavailable (Jibson, 1985).

Static (Aseismic) Slope Stability Analysis

Idealized Pre-Landslide Bluff Model. To analyze the long-term stability of the bluffs at the Stewart and Campbell sites, we constructed idealized models of the pre-landslide

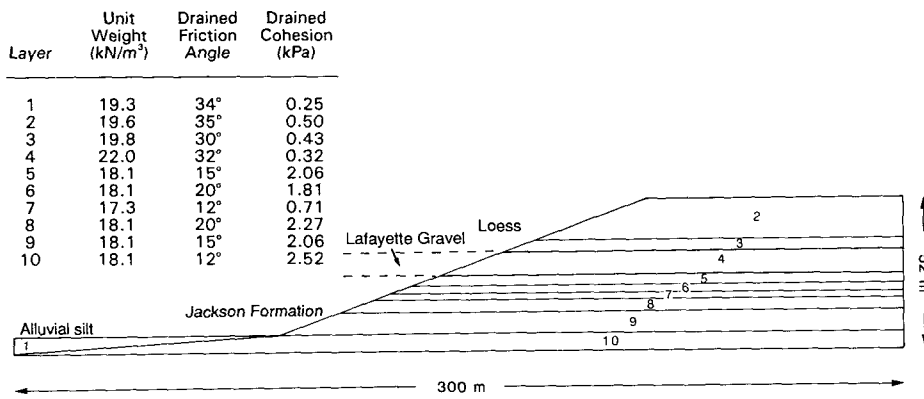| Layer	Unit Weight (kN/m³)	Drained Friction Angle	Drained Cohesion (kPa)
1	19.3	34°	0.25
2	19.6	35°	0.50
3	19.8	30°	0.43
4	22.0	32°	0.32
5	18.1	15°	2.06
6	18.1	20°	1.81
7	17.3	12°	0.71
8	18.1	20°	2.27
9	18.1	15°	2.06
10	18.1	12°	2.52

Figure 5. Idealized model of pre-landslide bluff at Stewart site in drained conditions.

bluffs for stability analysis. Undisturbed bluffs adjacent to the slides were examined to estimate the pre-landslide slope morphology. Stratigraphic data from the drilling were used to model subsurface conditions for two-dimensional analysis.

Geotechnical properties of the stratigraphic layers in the model were assigned using the results of the shear-strength tests; layers where no shear-strength tests were performed were assigned strengths based on stratigraphic and index-property correlation with layers where strengths were measured (Jibson, 1985). Strengths measured from direct and triaxial shear tests typically differ somewhat because the tests induce different failure geometries and stress conditions; to model the worst-case condition, the lowest shear strengths tested by either method are assigned to the layers in the model.

Figure 5 shows the idealized model of the pre-landslide bluff at the Stewart site in drained conditions and the geotechnical properties of each layer defined. The bluff is 45 m high as measured from the profile (Fig. 3). Undisturbed bluffs adjacent to the Stewart slide slope about 20° and have simple, uniformly sloping faces. Their profiles can be approximated by two horizontal lines representing the base and top of the bluff connected by a straight line-segment dipping 20° that represents the bluff face. The stratigraphy of the pre-landslide bluff is best illustrated in hole R-1 (Fig. 3), because this hole was placed above the scarp of the Stewart slide in intact material. In the plane of the model, the beds probably are horizontal because the bluff faces north, whereas the local dip of the Jackson Formation is to the west and is no more than a few degrees. The bluffs in the area have a thin veneer of loess, but this would have no significant effect on slope stability, and so the model shows each unit exposed in the bluff face.

Figure 6 shows the model of the pre-landslide bluff in drained conditions for the Campbell site. The intact bluff adjacent to the Campbell slide has an average slope of about 15°, and the profile (Fig. 4) indicates a bluff height of 55 m. The structure of the bluff at the Campbell site is somewhat different than that at the Stewart site because the strata dip out of the bluff face at about 5°. Fewer layers are defined for the Campbell slide because drilling results indicate that formations at this site are more uniform.

Ground-Water Conditions. Lack of published data makes modeling ground-water conditions along the bluffs difficult. Several potential ground-water conditions were analyzed (Fig. 7): (1) a water table at the top of the bluff, with seepage along the entire bluff face (the most critical situation); (2) a water table at the top of the Lafayette Gravel, with seepage on the bluff face only below this level; (3) a water table at the top of the Jackson Formation; (4) a water table at the base of the bluffs (the least critical situation); and (5) a water table sloping upward from the base of the bluffs to the top of the Jackson, and a second water table perched on the relatively impermeable Jackson Formation that satu-
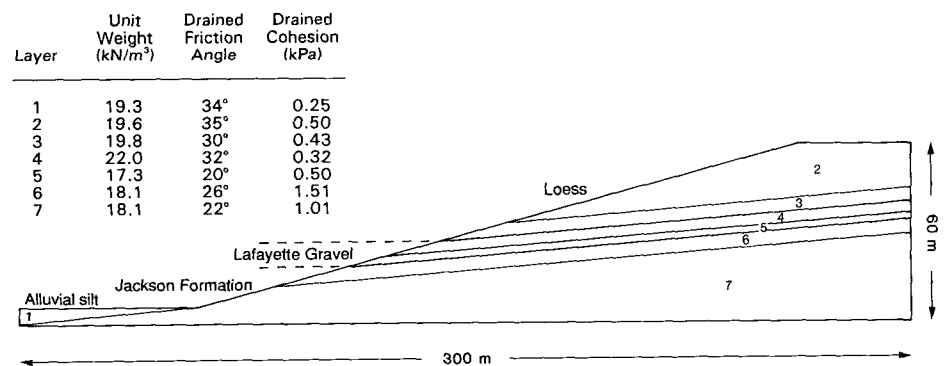
rates the Lafayette Gravel. Because of the topography of the area and the hydraulic properties of the bluff materials, the first condition is a more critical situation than can realistically exist in the bluffs and thus provides a worst-case bounding condition. Local hydrologists and geologists who have unpublished water-level data from wells along the bluffs (Robert Davis, Army Corps of Engineers, 1983, oral commun.; William Parks, U.S. Geol. Survey, 1983, oral commun.) indicate that condition 5 is the most likely.

Method of Stability Analysis. We used the computer program STABL (Siegel, 1978) to determine the stability of the modeled bluffs in aseismic conditions. STABL searches for the most critical failure surface by randomly generating circular, wedge-shaped, or irregular slip surfaces and calculating the factor of safety[1] for each randomly generated surface using the simplified Janbu method of slices (Siegel, 1978). The program plots the ten most critical surfaces of each type along with their factors of safety. STABL also calculates safety factors for slip surfaces having predetermined geometries.

The location of the actual failure surfaces were estimated from drilling data and from the surface geometry of the landslides; safety factors were calculated for these surfaces in each ground-water scenario. STABL generated a wide variety of circular and irregular surfaces, and wedge-shaped surfaces were generated in each layer of the Jackson Formation and Lafayette Gravel because the landslide geometries and drilling data indicate that the shear surfaces are beneath the loess.

---

[1]The factor of safety (*FS*) is the ratio of the sum of the resisting forces that act to inhibit slope movement to the sum of the driving forces that tend to cause movement. Slopes having factors of safety greater than 1.0 are thus stable; those having factors of safety less than 1.0 should move.

Layer	Unit Weight (kN/m³)	Drained Friction Angle	Drained Cohesion (kPa)
1	19.3	34°	0.25
2	19.6	35°	0.50
3	19.8	30°	0.43
4	22.0	32°	0.32
5	17.3	20°	0.50
6	18.1	26°	1.51
7	18.1	22°	1.01

Figure 6. Idealized model of pre-landslide bluff at Campbell site in drained conditions.

Most likely ground-water condition

Perched

Loess

Lafayette Gravel

Alluvial silt

Jackson Formation

Alternate ground-water conditions

Loess

Lafayette Gravel

Alluvial silt
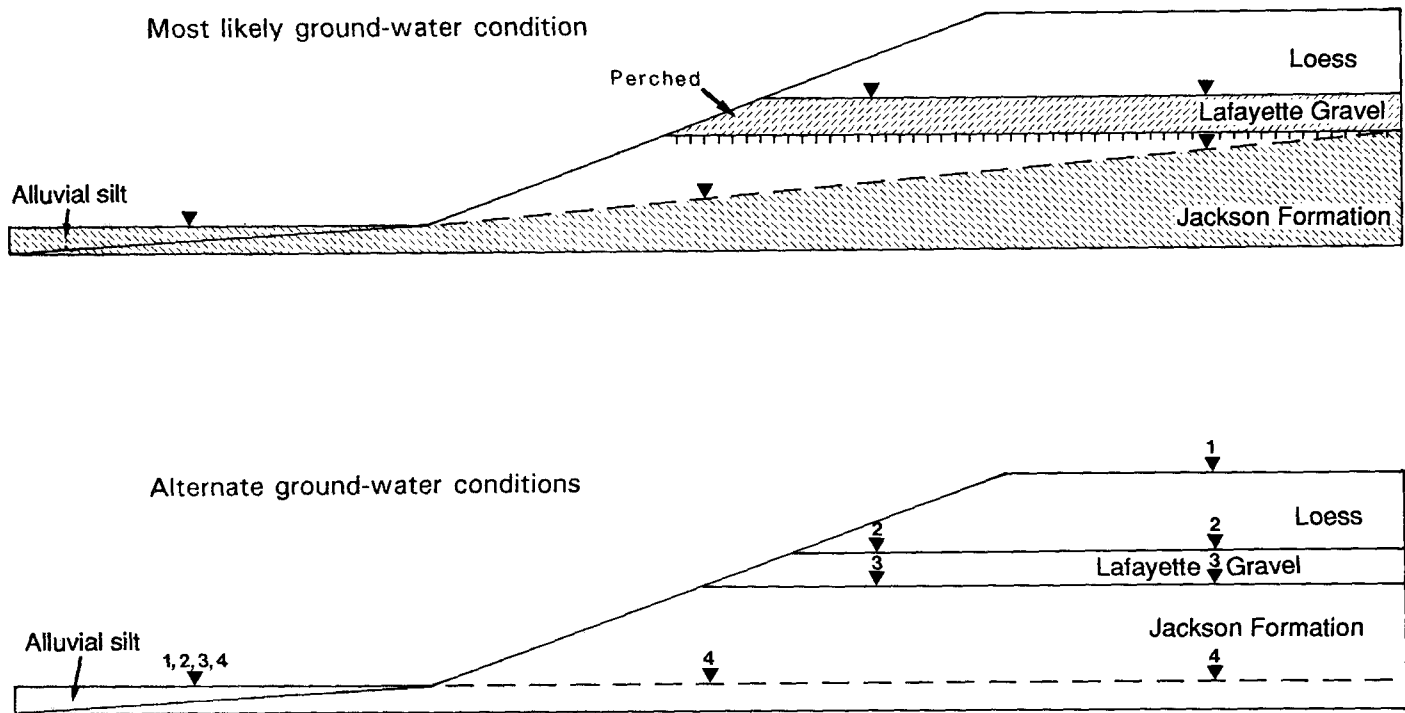
1,2,3,4

Jackson Formation

Figure 7. Ground-water conditions modeled in the slope-stability analysis. Upper drawing shows most likely ground-water conditions, lower drawing shows four other possible ground-water conditions; inverted triangles indicate piezometric surfaces for various ground-water conditions (1–4) described in text.

Analyses of circular failures assume that the entire slip surface fails in shear through all stratigraphic units; analyses of wedge-shaped surfaces that extend into the Jackson Formation assume that the loess and Lafayette Gravel fail in tension.

Results of Static Slope Stability Analysis. Determining the stability of the bluff from the factor of safety requires some judgment. Gedney and Weber (1978) recommended that engineered slopes have safety factors between 1.25 and 1.50. We use this range as the criterion to evaluate slope stability: between FS 1.00 and 1.25, slopes are considered marginally stable; between FS 1.25 and 1.50, slopes are considered stable; and above FS 1.50, slopes are considered very stable.

Results of the drained stability analyses of the Stewart and Campbell landslides are summarized in Table 1. For the Stewart site, the lowest factor of safety in the most critical ground-water situation is 1.32, which indicates that the bluff there is stable in aseismic conditions even in the most critical ground-water condition. In the most likely ground-water condition, the minimum factor of safety at the Stewart site is 1.82: the bluff is very stable. The factor of safety of the actual failure surface in the most likely ground-water condition is 1.88. For the Campbell site, the

minimum factor of safety in the most critical ground-water situation is 1.30, also in the stable range. In the most likely ground-water situation, the minimum factor of safety is 2.05, in the very stable range.

Our analyses indicate that an artesian pie-

zometric surface tens of meters above ground level at the top of the bluff would be needed to reduce the factor of safety to 1.0 at both sites. Such an artesian condition is implausible because (1) the regional geology and topography preclude such a condition, and (2)

TABLE 1. STATIC FACTORS OF SAFETY FROM STABILITY ANALYSES OF THE STEWART AND CAMPBELL LANDSLIDES IN DRAINED CONDITIONS

Type of failure surface	Base of bluff	Location of piezometric surface			Sloped and perched
		Top of Jackson Fm.	Top of Lafayette Gr.	Top of bluff	
Stewart landslide					
Circular	1.90	1.66	1.61	1.35	1.82
Irregular	1.95	1.69	1.64	1.32	1.87
Wedge, layer 5	4.06	3.98	3.76	2.83	4.03
Wedge, layer 6	4.24	4.03	3.80	2.79	4.23
Wedge, layer 7	2.46	2.28	2.14	1.47	2.45
Wedge, layer 8	3.81	3.39	3.23	2.51	3.72
Wedge, layer 9	2.83	2.48	2.38	1.88	2.71
Wedge, layer 10	2.40	2.10	2.03	1.68	2.25
Actual surface	1.96	1.73	1.67	1.40	1.88
Campbell landslide					
Circular	2.33	1.77	1.66	1.35	2.05
Irregular	2.40	1.82	1.71	1.35	
Wedge, layer 5	2.44	2.40	2.17	1.30	2.41
Wedge, layer 6	3.32	2.99	2.78	1.96	3.33
Wedge, layer 7	2.41	1.87	1.76	1.32	2.09
Actual surface	2.88	2.86	2.60	1.53	2.75

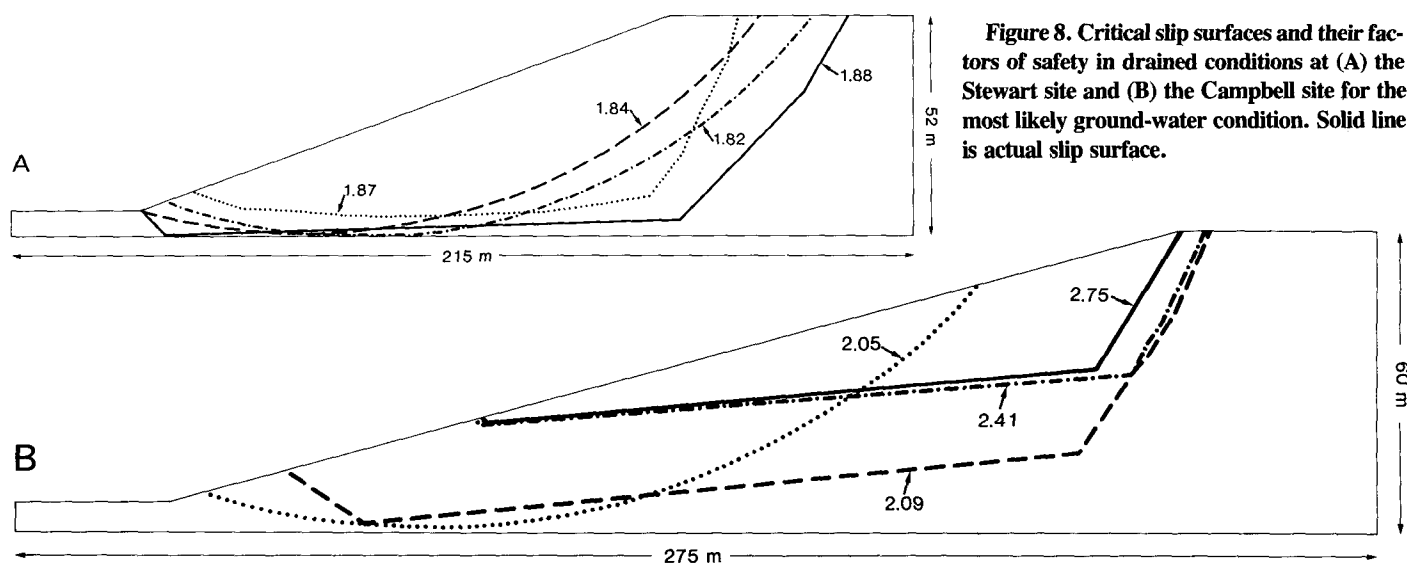*Note:* most critical surface for each ground-water condition shown in bold type.

Figure 8. Critical slip surfaces and their factors of safety in drained conditions at (A) the Stewart site and (B) the Campbell site for the most likely ground-water condition. Solid line is actual slip surface.

a piezometric surface far above the bluff top that dips steeply to the base of the bluff is physically unrealistic. Thus, within the limitations of our data and model, it appears highly improbable that these landslides could have formed aseismically in any conceivable ground-water conditions.

Figure 8 shows the locations of the most critical slip surfaces of various shapes and of the actual slip surfaces for the Stewart and Campbell slides. For the Stewart site, all of the surfaces have grossly similar shapes, but the randomly generated surfaces all lie well above the actual failure surface. For the Campbell site, the two most critical slip surfaces lie well below the actual surface and have factors of safety much lower than the actual surface and its adjacent randomly generated surface. This disparity between the most critical randomly generated slip surfaces and the actual surfaces also suggests that the existing landslides at the Stewart and Campbell sites did not form in aseismic, drained conditions.

Dynamic (Seismic) Slope Stability Analysis

We used the dynamic displacement analysis developed by Newmark (1965), now used widely in engineering practice (Seed, 1979), to evaluate the seismic stability of the bluffs. Newmark's method models a landslide as a rigid friction block of known critical acceleration—the acceleration required to overcome frictional resistance and initiate sliding—on an inclined plane. The analysis calculates the cumulative displacement of the block as it is
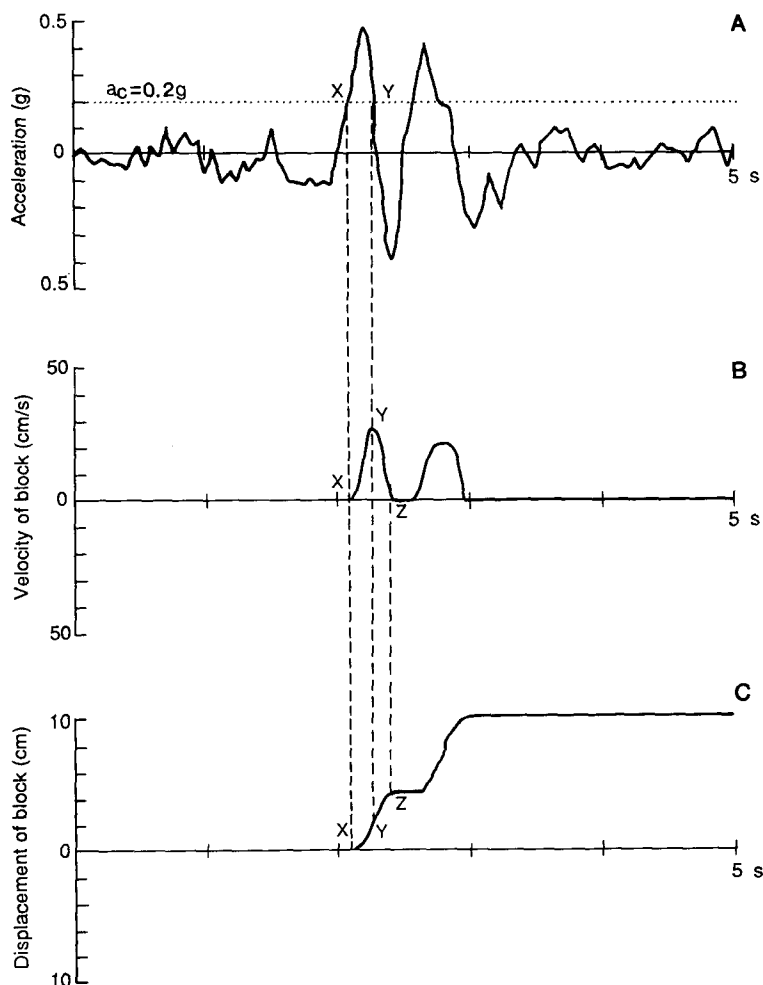

Figure 9. Demonstration of the Newmark-analysis algorithm (adapted from Wilson and Keefer, 1983). Points X, Y, and Z are discussed in text. A. Strong-motion record with critical acceleration (dotted line) superposed. B. Velocity of landslide block versus time. C. Displacement of block versus time.

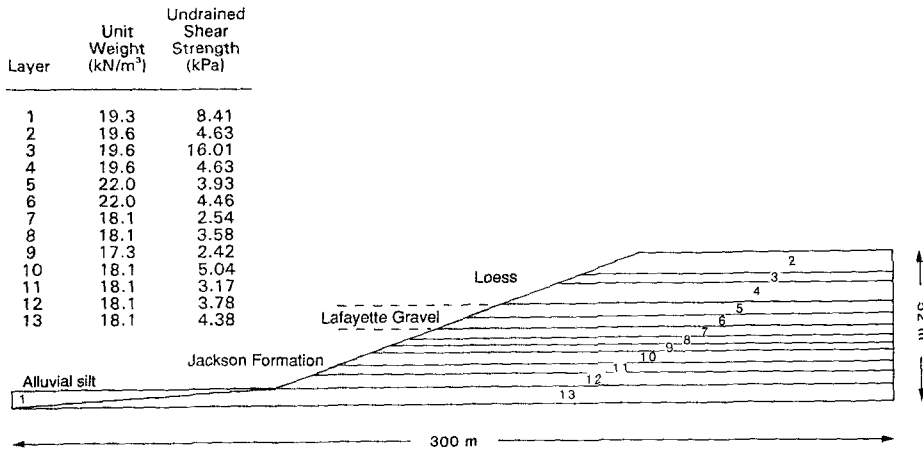| Layer	Unit Weight (kN/m³)	Undrained Shear Strength (kPa)
1	19.3	8.41
2	19.6	4.63
3	19.6	16.01
4	19.6	4.63
5	22.0	3.93
6	22.0	4.46
7	18.1	2.54
8	18.1	3.58
9	17.3	2.42
10	18.1	5.04
11	18.1	3.17
12	18.1	3.78
13	18.1	4.38

Figure 10. Idealized model of pre-landslide bluff at Stewart site in undrained conditions.

subjected to the effects of an earthquake acceleration-time history, and the user judges the significance of the displacement.

Laboratory model tests (Goodman and Seed, 1966) and analysis of earthquake-induced landslides (Wilson and Keefer, 1983) confirm that Newmark's method fairly accurately predicts slope displacements if slope geometry and soil properties are known and earthquake ground accelerations can be estimated. Newmark's method is a significant improvement over traditional pseudostatic stability analysis, which defines any exceedence of the critical acceleration, no matter how brief, as failure.

Newmark (1965) showed that the critical acceleration is a simple function of the static factor of safety and the landslide geometry; it can be expressed as

$$a_c = (FS - 1)g \sin \alpha, \quad (1)$$

where a_c is the critical acceleration in terms of g, the acceleration due to Earth's gravity; FS is the static factor of safety; and α is the angle (herein called the thrust angle) from the horizontal that the center of mass of the potential landslide block first moves.

We used the algorithm developed by Wilson and Keefer (1983) to apply Newmark's method. This algorithm allows both downslope and upslope displacement by explicitly accounting for the asymmetrical sliding resistance of a slope. In most cases, the upslope resistance is so great that no upslope displacement can occur, but landslides on low-angle slopes can experience pulses of upslope displacement, which are accounted for in this algorithm. Figure 9A shows a strong-motion record having a hypothetical a_c of 0.2 g superposed. To the left of point X (Fig. 9), the accelerations are less than a_c, and no land-

slide displacement occurs. To the right of point X, those parts of the strong-motion record lying above a_c are integrated over time to derive a velocity profile of the block. Integration begins at point X, and the velocity increases to point Y, the maximum velocity for this pulse. Past point Y, the ground acceleration drops below a_c, but the block continues to move because of its inertia. Frictional resistance and ground motion in the opposite direction decelerate the block until it comes to rest at point Z. All pulses of ground motion exceeding a_c are similarly integrated to yield a velocity profile (Fig. 9B), which, in turn, is integrated to yield a cumulative displacement profile of the landslide block (Fig. 9C).

Conducting a Newmark analysis requires three pieces of information: the static factor of safety and the thrust angle of the potential landslide, both needed to calculate the critical acceleration, and an earthquake acceleration-time history.

Factor of Safety. During earthquakes, slope materials behave in an undrained manner; thus, layered models of the bluffs in undrained conditions were constructed. Because undrained shear strength depends in large part on consolidation stress, layers of approximately similar thickness were constructed that reflect the increase in shear strength with depth even for relatively homogeneous materials.

Different shear-strength parameters were used for various layers depending on the ground-water conditions. For the Lafayette Gravel and the loess, drained strengths were used above the water table, undrained strengths below the water table. The Jackson Formation was considered saturated in all conditions because of its high clay content and consequent low permeability, and undrained shear strengths were used in all cases. The high undrained shear strength of the cemented loess layer makes the situation where the water table is at the top of the bluffs less critical than other situations.

STABL was used to generate potential failure surfaces and to determine the most critical failure surfaces in the same manner as described above for the drained stability analysis. Figures 10 and 11 show the undrained bluff models for the Stewart and Campbell sites, respectively; unit weights and undrained shear strengths for each layer are shown. Table 2 summarizes the results of the undrained stability analyses. The lowest factors of safety for the Stewart and Campbell sites are 1.53 and 1.32, respectively; thus, both bluff models are statically stable in undrained conditions.

Figure 12 shows the locations of the critical undrained failure surfaces for the Stewart and Campbell sites in the most likely ground-water condition. For the Campbell slide, the

Layer	Unit Weight (kN/m³)	Undrained Shear Strength (kPa)
1	19.3	8.41
2	19.6	16.01
3	19.8	4.63
4	22.0	4.33
5	17.3	1.26
6	18.1	2.87
7	18.1	3.40
8	18.1	3.75
9	18.1	4.10

Figure 11. Idealized model of pre-landslide bluff at Campbell site in undrained conditions.

TABLE 2. STATIC FACTORS OF SAFETY FROM STABILITY ANALYSES OF THE STEWART AND CAMPBELL LANDSLIDES IN UNDRAINED CONDITIONS

Type of failure surface	Base of bluff	Location of piezometric surface			Sloped and perched
		Top of Jackson Fm.	Top of Lafayette Gr.	Top of bluff	
Stewart landslide					
Circular	1.72	1.72	1.64	**1.99**	1.62
Irregular	**1.64**	**1.64**	1.55	2.16	**1.53**
Wedge, layer 5	2.81	2.81	2.50	3.59	2.49
Wedge, layer 6	3.23	3.23	2.96	3.84	2.93
Wedge, layer 7	2.19	2.19	1.99	2.81	1.97
Wedge, layer 8	3.18	3.18	3.05	3.57	3.02
Wedge, layer 9	2.00	2.00	1.89	2.41	1.87
Wedge, layer 10	1.99	1.99	1.88	2.25	1.87
Actual surface	1.74	1.74	1.66	2.12	1.65
Campbell landslide					
Circular	1.90	1.90	1.79	2.55	1.79
Irregular	1.79	1.79	1.74	3.12	1.74
Wedge, layer 5	**1.44**	**1.44**	**1.32**	3.68	**1.32**
Wedge, layer 6	1.85	1.85	1.76	3.19	1.76
Wedge, layer 7	1.84	1.84	1.77	2.97	1.77
Wedge, layer 8	1.76	1.76	1.71	2.60	1.71
Wedge, layer 9	1.67	1.67	1.64	**2.39**	1.64
Actual surface	2.63	2.63	1.57	5.64	1.57

Note: most critical surface for each ground-water condition shown in **bold** type.

most critical surface, a wedge failure in layer five, coincides almost exactly with the actual failure surface. For the Stewart slide, all of the slip surfaces, including the actual failure surface, plot very close to one another and have similar factors of safety. Both circular surfaces have large radii and approximate planar basal shear surfaces. The landslide geometry suggests (Fig. 3) that translatory movement likely occurred along a weak layer within the Jackson Formation; therefore, a wedge failure in one of the deeper layers might have been expected to produce the lowest factor of safety. Although a thin, weaker layer that failed and was not detected in the drill holes could possibly exist in the Jackson Formation, the proximity of the actual failure surface to the most critical failure surfaces generated by STABL indicates that the model agrees closely with observations.

The fact that the most critical computer-generated surfaces closely parallel the actual failure surfaces shows that the bluff models are realistic and that the Stewart and Campbell landslides are more likely to have failed in undrained conditions than in drained conditions.

Thrust Angle. The thrust angle is the direction that the center of gravity of the slide mass moves when displacement first occurs. For a planar slip surface parallel to the slope face (an infinite slope), this angle is the slope angle. For rotational movement, Newmark (1965) showed that the thrust angle is the angle between the vertical and a line segment connecting the center of gravity of the slide mass and the center of the slip circle.

Geometric constructions in Figure 12 show thrust angles of 15°–16° for the most critical surfaces of the Stewart slide. The thrust angle of the actual surface is difficult to estimate because of its irregular shape. We calculated an average inclination for the actual failure surface by weighting the inclinations of its component line segments by their relative lengths, which yields an angle of 16°, consistent with that of the other generated surfaces.

For the Campbell slide, the thrust angle is the inclination of the basal shear surface along which sliding occurred in layer five. The simple morphology of the slide and the coincidence of the most critical slip surface with the actual one justify this approach. Layer five dips 5°; this is used as the thrust angle. Anecdotal evidence (B. R. Clark, Leighton and Associates, 1992, written commun.) suggested that Newmark's method may overestimate landslide displacements at such low thrust angles, but we know of no physical reason for this. Indeed, Newmark's (1965) original work was intended in part to model dams sliding horizontally on their bases.

Earthquake Acceleration-Time History. Choosing a strong-motion record to represent the ground motions from the 1811–1812 earthquakes is difficult because most available records are for California earthquakes, which probably differ in some respects from large earthquakes in the central United States (Nuttli, 1983). Dif-

ferences in the propagation of strong ground motion, however, may not be as great as previously believed and appear to be significant only at great epicentral distances (>150 km) for very large earthquakes (Hanks and Johnston, 1992). Estimating ground-motion characteristics of the 1811–1812 earthquakes at the Stewart and Campbell sites and comparing these estimates with existing earthquake records provide a basis for choosing an input ground motion. Peak ground acceleration (*PGA*), duration, and shaking intensity are used for this comparison.

Nuttli and Herrmann (1984) used instrumental data from several central United States earthquakes to develop the following equation to relate mean horizontal *PGA* for soil sites in the central United States to earthquake magnitude and source distance:

$$\log \hat{a} = 0.57 + 0.50 \, m_b - 0.83 \log (R^2 + h^2)^{1/2} - 0.00069 \, R \quad (2)$$

where $\hat{a}$ is the *PGA* in centimeters per second squared, m_b is the body-wave magnitude, R is the epicentral distance in kilometers, and h is the focal depth in kilometers. For the 23 January and 7 February 1812 earthquakes, Nuttli's (1973) estimated epicenters (see Fig. 1) and magnitudes (m_b 7.1 and 7.4, respectively) are used to calculate epicentral distance. For the 16 December 1811 earthquake, Obermeier's (1989) analysis of the distribution of earthquake-triggered liquefaction effects indicates an epicenter about 15 km southwest of Nuttli's estimated location; we use this location and Nuttli's (1973) estimated magnitude (m_b 7.2). We use 20 km, the approximate maximum depth of instrumentally recorded earthquakes in the seismic zone, for the focal depth. These input parameters yield *PGA* values at the Stewart and Campbell sites between about 0.4 g and 0.7 g (Table 3).

PGA measures only a single point in an acceleration-time history and is thus a rather crude single measure of earthquake shaking intensity. A more quantitative measure of total shaking intensity developed by Arias (1970) is useful in seismic hazard analysis and correlates well with distributions of earthquake-induced landslides (Harp and Wilson, 1989). Arias intensity is the integral over time of the square of the acceleration, expressed as

$$I_a = \pi/2g \int [a(t)]^2 dt \quad (3)$$

where I_a is the Arias intensity, expressed in units of velocity, and $a(t)$ is the ground acceleration as a function of time.

Wilson and Keefer (1985) developed a simple relationship between Arias intensity, earthquake magnitude, and source distance:

$$\log I_a = M - 2\log R - 4.1 \qquad (4)$$

where I_a is in meters per second, M is moment magnitude, and R is earthquake source distance in kilometers. Equation 4 was developed from California earthquakes and may slightly underestimate shaking intensity in the central United States. Table 3 shows Arias intensities estimated from equation 4 using moment-magnitude esti-

mates from Hamilton and Johnston (1990) and source distances based on earthquake locations as described above.

Arias intensity also correlates closely with combined PGA and duration. R. C. Wilson (U.S. Geol. Survey, 1988, written commun.) developed an empirical equation using 43 strong-motion records to predict Arias intensity from PGA and duration:

$$I_a = 0.9\ T\hat{a}^2 \qquad (5)$$

where I_a is in meters per second, $\hat{a}$ is the PGA in g's, and T is the duration (hereafter called

Dobry duration) in seconds, defined by Dobry and others (1978) as the time needed to build up the central 90% of the Arias intensity. Estimating Arias intensities using this method requires an estimate of the duration of strong shaking in 1811–1812.

Because duration is a difficult parameter to estimate, we use a variety of methods and compare the results to estimate a probable range of durations of strong shaking. Dobry and others (1978) proposed an empirical relationship between duration and magnitude:

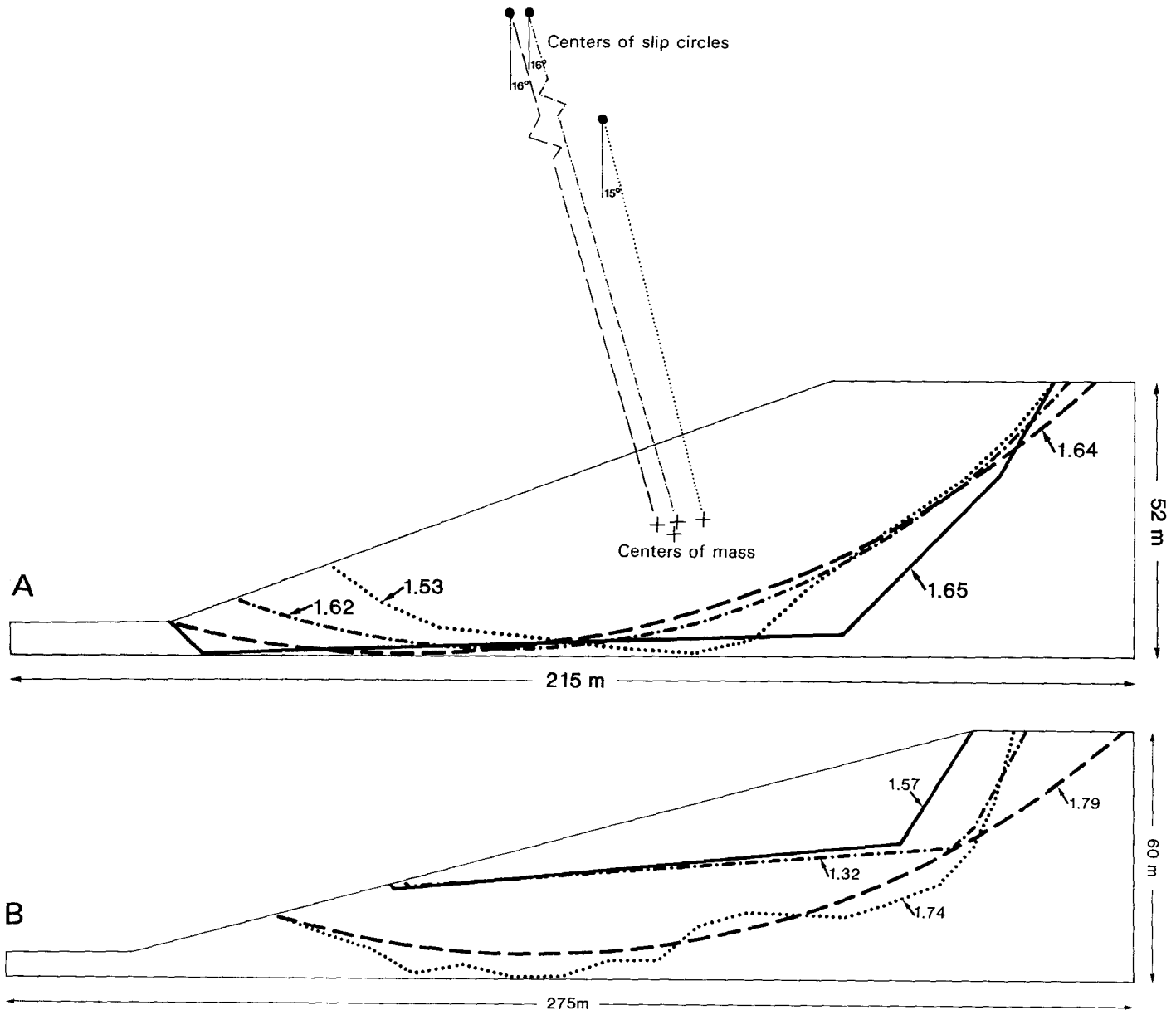$$\log T = 0.432M - 1.83 \qquad (6)$$

Figure 12. Critical slip surfaces and their factors of safety in undrained conditions at (A) the Stewart site and (B) the Campbell site for the most likely ground-water condition. Geometric constructions to determine the thrust angle of the Stewart slide are shown.

TABLE 3. STRONG-MOTION RECORDS USED TO MODEL GROUND SHAKING FROM THE 1811–1812 EARTHQUAKES AT THE STEWART AND CAMPBELL LANDSLIDES

Earthquake Recording site, component	M	R (km)	$\hat{a}$ (g)	T (s)	I_a (m/s)	D_N (cm)
Stewart landslide						
16 Dec 1881 New Madrid, Mo.,					2.7*	
Stewart landslide site (estimated)	8.2	68	0.39	20–40	2.7–5.5†	
• 15 Oct 1979 Imperial Valley, Calif.,						
El Centro differential array, 360°	6.5	7	0.49	6.6	2.1	6–8
• 24 Nov 1987 Superstition Hills, Calif.,						
Superstition Mountain site 8, 135°	6.5	6	0.90	12.2	6.8	22–25
23 January 1812 New Madrid, Mo.,					17.4*	
Stewart landslide site (estimated)	8.1	24	0.74	18–40	8.9–19.7†	
• 9 Feb 1971 San Fernando, Calif.,						
Pacoima Dam, 164°	6.6	3	1.22	6.7	9.1	49–55
• 16 Sep 1978 Tabas, Iran, 74°	7.4	3	0.71	16.1	10.0	39–44
7 Feb 1812 New Madrid, Mo.,					8.2*	
Stewart landslide site (estimated)	8.3	44	0.71	25–40	11.3–18.1†	
• 24 Nov 1987 Superstition Hills, Calif.,						
Superstition Mountain site 8, 135°	6.5	6	0.90	12.2	6.8	22–25
• 16 Sep 1978 Tabas, Iran, 74°	7.4	3	0.71	16.1	10.0	39–44
Campbell landslide						
16 Dec 1811 New Madrid, Mo.,					3.6*	
Campbell landslide site (estimated)	8.2	59	0.44	20–40	3.5–7.0 †	
• 24 Nov 1987 Superstition Hills, Calif.,						
Parachute test site, 315°	6.5	1	0.52	10.9	3.0	121–202
• 24 Nov 1987 Superstition Hills, Calif.,						
Superstition Mountain site 8, 135°	6.5	6	0.90	12.2	6.8	130–208
23 Jan 1812 New Madrid, Mo.,					13.7*	
Campbell landslide site (estimated)	8.1	27	0.70	18–40	7.9–17.6†	
• 24 Nov 1987 Superstition Hills, Calif.,						
Superstition Mountain site 8, 135°	6.5	6	0.90	12.2	6.8	130–208
• 16 Sep 1978 Tabas, Iran, 74°	7.4	3	0.71	16.1	10.0	262–453
7 Feb 1812 New Madrid, Mo.,					6.6*	
Campbell landslide site (estimated)	8.3	49	0.65	25–40	9.5–15.2†	
• 24 Nov 1987 Superstition Hills, Calif.,						
Superstition Mountain site 8, 135°	6.5	6	0.90	12.2	6.8	130–208
• 16 Sep 1978 Tabas, Iran, 74°	7.4	3	0.71	16.1	10.0	262–453

Note: characteristics of the 1811–1812 earthquakes estimated as described in text. All strong-motion records are from U.S. Geological Survey recording stations except for the Tabas, Iran, record (Hadley and others, 1983). M is moment magnitude (estimates for the 1811–1812 earthquakes from Hamilton and Johnston, 1990); $\hat{a}$ is peak ground acceleration; T is duration of strong shaking as defined by Dobry and others (1978); I_a is Arias (1970) intensity; D_N is Newmark (1965) displacement (range shown covers range of critical accelerations discussed in text).
*Estimated using equation 4.
†Estimated using equation 5.

where T is Dobry duration in seconds and M is unspecified earthquake magnitude (probably local magnitude, M_L). In the magnitude range of interest, M_L values are about 0.1 magnitude points greater than m_b values. Thus, equation 6 yields Dobry durations of 20, 18, and 25 s, respectively, for the three 1811–1812 earthquakes (Table 3).

Krinitzsky and Marcuson (1983) plotted bracketed durations (time between first and last acceleration pulses above 0.05 g) against Modified Mercalli Intensity (MMI) for different site conditions. Although few data plot in the MMI X–XI range of interest here, their curves suggest a bracketed duration between 40 and 60 s. Bracketed durations at the 0.05-g level are about 50% longer than Dobry durations in the magnitude range of interest (Dobry and others, 1978); thus, the lower value of 40 s is a reasonable estimate of the maximum Dobry duration for all three 1811–1812 earthquakes using this method.

We also examined estimated seismic source durations to verify that the ranges es-timated above are realistic. Somerville and others (1987) developed theoretical and empirical relationships between earthquake moment and source duration for earthquakes in eastern North America. Using moment estimates for the 1811–1812 events of $10^{28.2}$–$10^{28.5}$ dyne-cm (A. C. Johnston, Memphis State Univ., 1991, written commun.) yields source durations of 26–33 s, within the ranges estimated above.

We applied equation 5 to the *PGA* values and the upper and lower bound durations estimated above to estimate Arias intensities at the Stewart and Campbell sites for the three 1811–1812 earthquakes. Resulting Arias intensity estimates are shown in Table 3. Estimates for the 16 December 1811 and 23 January 1812 earthquakes using equation 4 are within the range of intensities estimated using equation 5, and intensity estimates for the 7 February 1812 earthquake are somewhat lower. Both methods thus provide compatible intensity estimates that can be used to characterize shaking conditions at the two sites.

Although strong motion has not been recorded for earthquakes in the magnitude range of the 1811–1812 events, several existing strong-motion records have shaking characteristics similar enough to estimated shaking characteristics of the 1811–1812 events to be useful. Availability of records only from earthquakes having smaller magnitudes generally necessitated using records having smaller source distances, which may affect the spectral composition of the shaking. We examined an extensive catalog of digitized strong-motion records, primarily from California earthquakes, and selected two records for each site for each of the three 1811–1812 earthquakes (a total of six records for each site). Records were selected to match, as closely as possible, the estimated range of Arias intensities and *PGA*'s from the 1811–1812 events so as to bracket the likely range of shaking conditions that actually occurred. None of the available strong-motion records has Arias intensities greater than 10 m/s; therefore, where estimated Arias intensities exceed this level, the available record having the greatest Arias intensity was used. Characteristics of the records selected compare well with those estimated for the Stewart and Campbell sites (Table 3).

Calculation of the Newmark Landslide Displacement. The static factor of safety from the undrained slope stability analysis and the thrust angle from the landslide geometry are combined in equation 1 to calculate the critical acceleration. The critical acceleration is then specified in the computer program that double integrates the strong-motion record to calculate the Newmark displacement.

The significance of the Newmark displacements must be judged in terms of the probable effect on the potential landslide mass. For example, Wieczorek and others (1985) used 5 cm as the critical displacement leading to general failure of landslides in San Mateo County, California; Keefer and Wilson (1989) used 10 cm as the critical displacement for coherent landslides in southern California. When displacements in this range occur, most soils lose a significant amount of their shear strength and are in a residual-strength condition. Laboratory shear-strength tests on samples from the Stewart and Campbell sites indicate that residual strength is reached after a total shear displacement of about 6 cm (Jibson, 1985); therefore, the 5- to 10-cm range is reasonable for these landslides. If this amount of displacement is exceeded, static factors of safety using residual strengths can be calculated to determine the stability of the landslide after the earthquake shaking ceases.

Results of Dynamic Analysis of Stewart Landslide. For the Stewart landslide, we calculated critical accelerations based on a thrust angle of 16° and on the factors of safety of the two circular slip surfaces in the perched and sloped ground-water condition (FS = 1.62, 1.64), because they most closely coincide with the actual surface and have the lowest factors of safety (Fig. 8). Equation 1 yields critical accelerations of 0.17–0.18 g for these input values. Newmark displacements were calculated for these two critical accelerations using the six strong-motion records listed in Table 3.

Results of the Newmark analyses are shown in Table 3. Displacements are between 6 and 55 cm and thus overlap the critical 5- to 10-cm range. Displacements generated by the model earthquakes for the 16 December 1811 event are between 6 and 25 cm; in this range, the likelihood of catastrophic failure is uncertain, but enough displacement probably occurred during this earthquake to at least partly reduce soil shear strength and thus reduce the critical acceleration of the slide mass in future earthquakes. The model earthquakes for the 23 January and 7 February 1812 events generated Newmark displacements of 22–55 cm, amounts that would undoubtedly reduce soil shear strengths to residual levels.

Static factors of safety for the Stewart slide were calculated using residual strengths in both drained and undrained conditions (Jibson, 1985); in all ground-water conditions, safety factors were much less than 1.0. Therefore, if the bluff soils reach residual strength, catastrophic failure is highly probable even without earthquake shaking. Because Newmark displacements in successive earthquakes are cumulative, the entire 1811–1812 sequence would have generated a minimum of about 1 m of displacement, which almost certainly would have reduced the strength of the bluff materials to residual levels and caused catastrophic failure.

Results of Dynamic Analysis of Campbell Landslide. We computed Newmark displacements of the Campbell slide using the following parameters: (1) the static factors of safety from the undrained analysis in the perched and sloped ground-water condition for the actual failure surface (FS = 1.57) and the most critical generated surface (FS = 1.32) (Fig. 8), (2) a thrust angle of 5°, and (3) earthquake acceleration-time histories from Table 3. The critical accelerations computed (eqn. 1) for the two failure surfaces are 0.03 and 0.05 g.

Displacements from the Newmark analysis are 121–453 cm (Table 3). Such large displacements almost certainly would lead to reduction of shear strength to residual levels.

The effect of the much lower critical acceleration of the Campbell slide is evident in the substantially larger Newmark displacements; any of the earthquakes modeled would generate large inertial displacements that would reduce soil strength to residual levels. Static slope stability analyses using residual strengths in both drained and undrained conditions all yield factors of safety well below 1.0; therefore, catastrophic failure is highly probable after large earthquake-induced displacements in the slope.

Summary of Stability Analyses

The static stability analyses of the Stewart and Campbell landslides show that failure in the absence of earthquake shaking is very unlikely even using minimum shear strengths in unrealistically high ground-water conditions. The dynamic analyses show that earthquake shaking similar to that in 1811–1812 would have induced large displacements probably leading to catastrophic failure.

WHAT IF SEISMIC CONDITIONS ARE UNKNOWN?

If we knew nothing about the ground shaking in 1811–1812, or if we did not even know if earthquakes had ever occurred in that region, could analysis of these landslides tell us anything of their possible origin? The static stability analyses clearly indicate that failure in aseismic conditions is highly unlikely, and an earthquake origin could be hypothesized on that basis alone. The dynamic analysis could then be used to estimate the minimum shaking intensities necessary to have caused failure.

Such an approach requires a general relationship between critical acceleration, Arias intensity, and Newmark displacement. To estimate the Newmark displacement associated with a given Arias intensity and critical acceleration, we selected 11 strong-motion records having Arias intensities between 0.2 and 10.0 m/s (Table 4), which span the range between the smallest shaking intensities that might cause landslide movement and the largest shaking intensities ever recorded. For each strong-motion record, we calculated the Newmark displacement for several critical accelerations between 0.02 and 0.40 g, the range of practical interest for most earthquake-induced landslides. The resulting data are plotted in Figure 13. Data points for each critical acceleration plot fairly linearly in the log-log space of Arias intensity versus Newmark displacement. Best-fit lines from regres-

sion models for each value of critical acceleration have excellent fits (R^2 values of 0.81–0.95), and the lines are approximately parallel and proportionately spaced, which suggests that a multivariate model of the following form would fit the data well:

$$\log D_N = A\log I_a + Ba_c + C \quad (7)$$

where D_N is Newmark displacement in centimeters, I_a is Arias intensity in meters per second, a_c is critical acceleration in g's, and A, B, and C are the regression coefficients. The resulting model has an R^2 of 0.87, and the coefficients all are significant above the 99.9% confidence level:

$$\log D_N = 1.460\log I_a - 6.642a_c + 1.546. \quad (8)$$

Figure 14 shows critical-acceleration lines derived from equation 8.

The threshold earthquake shaking intensity necessary to trigger the Stewart and Campbell landslides can be estimated by judging the amount of Newmark displacement (the critical displacement) that would reduce shear strength on the failure surface to residual levels and lead to catastrophic failure. As discussed above, critical displacements of about 10 cm are probably realistic for these types of slides, based on previous studies (Wieczorek and others, 1985; Wilson and Keefer, 1985; Keefer and Wilson, 1989), laboratory shear-strength testing of soil samples from our sites (Jibson, 1985), and field studies of landslides in the region (Jibson and Keefer, 1988). Inserting a displacement value of 10 cm and the

TABLE 4. STRONG-MOTION RECORDS SELECTED FOR ANALYSIS

Earthquake Recording site, component	M	$\hat{a}$ (g)	T (s)	I_a (m/s)
15 Oct 1979 Imperial Valley, Calif., Coachella Canal, station 4, 135°	6.5	0.13	10.4	0.20
6 Aug 1979 Coyote Lake, Calif., Coyote Creek, San Martin, 250°	5.8	0.21	3.8	0.25
21 Jul 1952 Kern County, Calif., Taft School, 111°	7.5	0.14	17.7	0.46
6 Aug 1979 Coyote Lake, Calif., Gilroy array, San Ysidro School, 270°	5.8	0.23	8.5	0.60
15 Oct 1979 Imperial Valley, Calif., Calexico Fire Station, 225°	6.5	0.28	11.1	0.86
1 Oct 1987 Whittier Narrows, Calif., Bulk Mail Center, 280°	6.0	0.45	5.5	1.23
15 Oct 1979 Imperial Valley, Calif., El Centro differential array, 360°	6.5	0.49	6.6	2.12
24 Nov 1987 Superstition Hills, Calif., Parachute test site, 225°	6.5	0.46	10.1	4.15
15 Oct 1979 Imperial Valley, Calif., Bonds Corner, 230°	6.5	0.79	9.8	6.00
9 Feb 1971 San Fernando, Calif., Pacoima Dam, 164°	6.6	1.22	6.7	9.08
16 Sep 1978 Tabas, Iran, 74°	7.4	0.71	16.1	9.96

Note: M is moment magnitude, $\hat{a}$ is peak ground acceleration, T is duration as defined by Dobry and others (1978), and I_a is Arias intensity. All strong-motion records are from USGS recording stations except for the Tabas, Iran, record (Hadley and others, 1983).
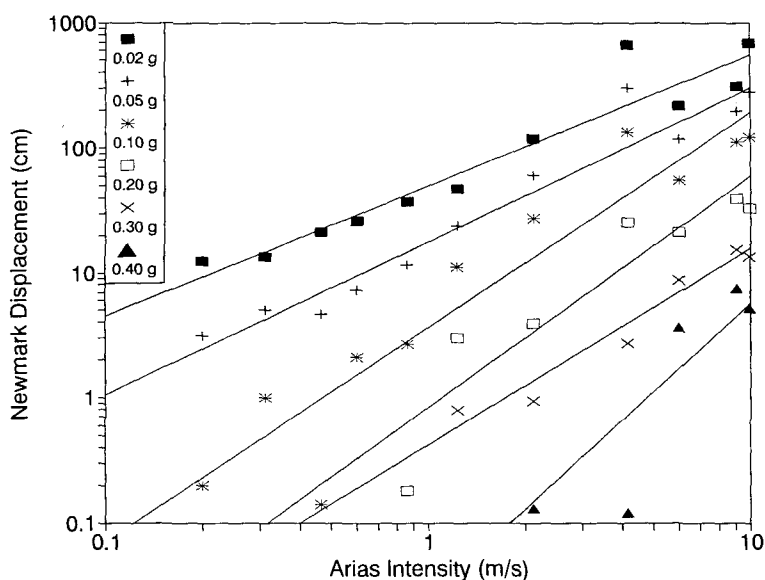
Figure 13. Newmark displacement as a function of Arias intensity for critical accelerations of 0.02–0.40 g. Best-fit regression lines for each critical acceleration shown.

critical accelerations of the Stewart (0.17–0.18 g) and Campbell (0.03–0.05 g) landslides into equation 8 yields a lower bound Arias intensity of about 2.6 m/s to trigger the Stewart slide and about 0.6 m/s to trigger the Campbell slide.

The threshold earthquake magnitude (M) needed to trigger these landslides can be estimated using equation 4. If we assume a minimum source distance of 5 km (the focal depth at the epicenter), the Arias intensities estimated above yield lower bound threshold moment magnitudes (M) of 5.9 for the Stewart landslide and 5.3 for the Campbell landslide. Lower bound threshold body-wave magnitudes (m_b) can be estimated using equations 2, 5, and 6 in combination, which yield lower bound m_b values of 5.8 for the Stewart slide and 5.4 for the Campbell slide.

DISCUSSION

Several damaging earthquakes have occurred in the New Madrid seismic zone since the 1811–1812 sequence. Nuttli (1982) described the 20 most damaging earthquakes since 1812 and estimated their locations and magnitudes. Could any of these more recent earthquakes have triggered the landslides we studied? We answer this question by using equation 8 to estimate the effects from these earthquakes at the Stewart and Campbell landslide sites.

We selected the earthquakes from Nuttli (1982) that would have produced the greatest shaking intensities at the Stewart and Camp-

bell sites. We selected the largest earthquake $(m_b = 6.2)$ and then eliminated all earthquakes of lower magnitudes that were farther from our sites. For earthquakes closer to our sites than the $m_b = 6.2$ event, we selected the next largest magnitude and eliminated all earthquakes of lesser magnitude that were farther from our sites. Using this iterative approach, we selected 3 of the 20 earthquakes that would have produced the greatest shaking intensities at the Stewart and Campbell sites.

We used equations 4 and 5 to estimate the range of possible Arias intensities that would have been produced from each of these earthquakes at each of our sites. Equation 4 requires the magnitude and distance, which are taken from Nuttli's (1982) estimates. Equation 5 requires knowing the *PGA* and the duration of strong shaking; we estimated the maximum *PGA* using equation 2 and the duration using equation 6. Table 5 shows characteristics of the three selected earthquakes and the estimated ranges of *PGA*'s and Arias intensities at the Stewart and Campbell sites. All of the earthquakes probably would have produced *PGA*'s at the Stewart site much lower than the critical acceleration necessary to initiate landslide movement (0.17–0.18 g); therefore, none of these earthquakes is likely to have triggered any landslide movement there. At the Campbell site, the estimated *PGA* values are all at or slightly above the critical acceleration (0.03–0.05 g), and thus we need to determine if the estimated Arias intensities would have been sufficient to generate enough displacement to cause failure.

Combining the greatest estimated Arias intensity for the Campbell site from Table 5 (0.077 m/s) with the range of critical accelerations for the Campbell slide (0.03–0.05 g) in equation 8 yields Newmark displacements of 0.4–0.5 cm, an order of magnitude smaller than the lower bound critical displacement levels of 5–10 cm required to cause catastrophic failure. Thus, we conclude that no earthquakes since 1812 are likely to have trig-
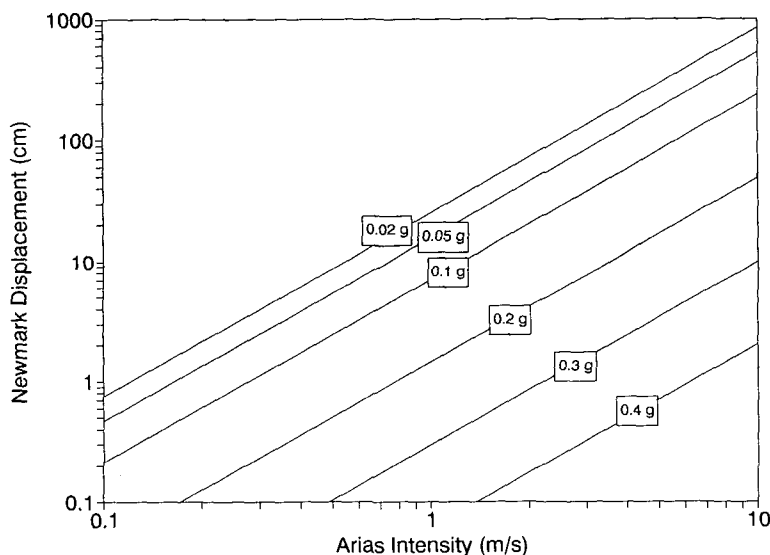

Figure 14. Critical acceleration contours derived from multivariate regression of Arias intensity and critical acceleration versus Newmark displacement (eqn. 8).

TABLE 5. MOST DAMAGING EARTHQUAKES SINCE 1811–1812

Date	m_b	M_L	M	T (s)	Stewart landslide				Campbell landslide			
					R (km)	$\hat{a}$ (g)	I_a^1 (m/s)	I_a^2 (m/s)	R (km)	$\hat{a}$ (g)	I_a^1 (m/s)	I_a^2 (m/s)
31 Oct 1895	6.2	6.6	6.8	10.5	96	0.09	0.077	0.054	103	0.09	0.077	0.047
4 Nov 1903	5.3	5.6	5.5	3.9	86	0.04	0.006	0.003	94	0.03	0.003	0.003
21 Aug 1905	5.0	5.4	5.4	3.2	75	0.03	0.003	0.004	82	0.03	0.003	0.003

Note: m_b is body-wave magnitude from Nuttli (1982); M_L is local magnitude, and M is moment magnitude, both converted from m_b as suggested by Heaton and others (1986); T is duration estimated from equation 6; R is epicentral distance to each site using locations from Nuttli (1982); $\hat{a}$ is peak horizontal ground acceleration estimated from Nuttli and Herrmann (1984); I_a^1 is Arias intensity estimated using equation 4; I_a^2 is Arias intensity estimated using equation 5.

gered catastrophic movement of the Campbell slide.

Equation 8 and Figure 13 can be applied to estimate the dynamic performance of any slope of known critical acceleration because they are derived from generic values of critical acceleration that are not site specific. Thus, several types of regional hazard analyses for earthquake-triggered landslides can be developed using equation 8. A common type of regional earthquake hazard analysis involves estimating the effects from a proposed model earthquake of given magnitude and location. In such a scenario-based hazard analysis, the seismic stability of slopes of known critical acceleration can be estimated by using (1) equation 4 to estimate the Arias intensity from the postulated earthquake magnitude and location and (2) equation 8 to calculate the Newmark displacement. An alternative approach is to use (1) equation 2 (or a similar attenuation equation appropriate for the region of interest) to estimate the *PGA*, (2) equation 6 to estimate the duration, (3) equation 5 to calculate the Arias intensity from the *PGA* and duration, and (4) equation 8 to calculate the Newmark displacement. Although microzonation of critical acceleration over a broad area is difficult, Wieczorek and others (1985) have documented a reasonable approach for regional analysis.

If critical displacements for slope materials in an area can be estimated using laboratory testing or field observations, then equation 8 can be used to estimate (1) the threshold Arias intensity required to initiate failure of slopes of given critical acceleration and (2) the critical acceleration below which slopes will fail for a given shaking intensity. These approaches can be applied in several ways to estimate regional seismic slope stability. This represents an incremental improvement over the previous methods, which assumed a uniform level of ground shaking throughout a region.

If the Stewart and Campbell landslides are typical of block slides and earth flows in the New Madrid region, then the shaking-intensity and magnitude thresholds discussed previously could be considered lower bound conditions for triggering large landslides of these types in future earthquakes. Thus, an Arias intensity of about 2.6 m/s, corresponding to a minimum M = 5.9 or m_b = 5.8 earthquake, would be necessary to trigger block slides similar to the Stewart slide. For earth flows similar to the Campbell slide, an Arias intensity of 0.6 m/s, corresponding to a minimum M = 5.3 or m_b = 5.4 earthquake, would be required. Obviously, larger earthquakes are required to trigger landslides at greater epicentral distances and across a large area.

In this paper, we have developed and successfully applied an approach for assessing the likelihood that a landslide or group of landslides of unknown origin was seismically triggered. The data and slope-stability models used all have inherent uncertainties, and so an analytical approach such as this can never, by itself, unequivocally prove the origin of a landslide. When used in conjunction with other types of field evidence, however, the approach developed in this paper can have important applications in paleoseismology. If field evidence and slope-stability analyses show that a group of landslides in a region is much more likely to have formed seismically than aseismically, an earthquake origin can be inferred. If such landslide features can be dated, a date for the postulated triggering earthquake can be determined. Dynamic analysis of such landslides can yield minimum shaking intensities that would have been required to trigger failure. In areas such as the central and eastern United States, where exposures of recent faults are absent or yield equivocal interpretations, groups of old landslides that can be shown to have been triggered by earthquake shaking might be used for paleoseismic dating. If more than one generation of such features exists, earthquake return periods could be established. The possibility of such an application exists in the New Madrid seismic zone, where we have

mapped many features of questionable origin, some of which may be an older, more eroded set of landslides (Jibson and Keefer, 1988).

SUMMARY AND CONCLUSIONS

Static and dynamic analyses of two large landslides that are representative of coherent block slides and earth flows in the New Madrid seismic zone show that neither is likely to have moved in the absence of earthquake shaking, even when minimum shear strengths and unrealistically high groundwater conditions are modeled. During earthquake shaking similar to that in 1811–1812, both probably would have experienced large displacements leading to catastrophic failure. Analysis of shaking intensities generated by the largest earthquakes since the 1811–1812 sequence indicates that no earthquakes since then are likely to have triggered the observed slide movement. These analyses are fully consistent with results from our previous studies (Jibson and Keefer, 1988, 1989), and considered together they lead us to conclude that the Stewart and Campbell landslides did, indeed, form during the 1811–1812 earthquakes.

Back calculations of threshold shaking intensities required to cause catastrophic failure indicates that earthquakes of m_b = 5.4 or M = 5.3 are required to trigger earth flows similar to the Campbell slide and that earthquakes of m_b = 5.8 or M = 5.9 are required to trigger coherent slides similar to the Stewart slide.

The approach for determining the likely conditions—seismic or aseismic—that triggered failure of these landslides can be applied to landslides in other areas. In some cases, it may be impossible to infer an earthquake origin for a landslide or group of landslides if failure in aseismic conditions cannot reasonably be ruled out. In cases where an earthquake origin can be supported for a landslide, establishing the age of the sliding will indicate the timing of the triggering earthquake. Back analysis of minimum shaking intensities can establish a lower bound magnitude for the triggering earthquake. Hence, the approach described in this paper can find useful application in paleoseismic studies.

The empirical relationship developed between Newmark displacement, Arias intensity, and critical acceleration also can be applied to a variety of seismic hazard problems related to slope instability. Specifically, if a model earthquake of designated location and magnitude is postulated, then the Newmark displacement of slopes of known critical acceleration can be estimated. If the critical dis-

placement is known, then the shaking intensity required to cause failure of a slope of known critical acceleration can be estimated, or, for a given shaking intensity, the critical acceleration below which slopes will fail can be estimated.

ACKNOWLEDGMENTS

REFERENCES CITED

Arias, A., 1970, A measure of earthquake intensity, *in* Hansen, R. J., ed., Seismic design for nuclear power plants: Cambridge, Massachusetts, Massachusetts Institute of Technology Press, p. 438–483.

Conrad, T. A., 1856, Observations on the Eocene deposit of Jackson, Miss., with descriptions of 34 new species of shells and corals: Philadelphia Academy of Natural Science, Proceedings, 1855, 1st ser., v. 7, p. 257–258.

Dobry, R., Idriss, I. M., and Ng, E., 1978, Duration characteristics of horizontal components of strong-motion earthquake records: Seismological Society of America Bulletin, v. 68, p. 1487–1520.

Fuller, M. L., 1912, The New Madrid earthquake: U.S. Geological Survey Bulletin 494, 119 p.

Gedney, D. S., and Weber, W. G., Jr., 1978, Design and construction of soil slopes, *in* Schuster, R. L., and Krizek, R. J., eds.,

Landslides—Analysis and control: National Academy of Sciences, Transportation Research Board, Special Report 176, p. 172–191.

Goodman, R. E., and Seed, H. B., 1966, Earthquake-induced displacements in sand embankments: American Society of Civil Engineers, Journal of the Soil Mechanics and Foundation Division, v. 92, no. SM2, p. 125–146.

Hadley, D. M., Hawkins, H. G., and Benuska, K. L., 1983, Strong ground motion record of the 16 September 1978 Tabas, Iran, earthquake: Seismological Society of America Bulletin, v. 73, no. 1, p. 315–320.

Hamilton, R. M., and Johnston, A. C., 1990, Tecumseh's prophecy—Preparing for the next New Madrid earthquake: U.S. Geological Survey Circular 1066, 30 p.

Hanks, T. C., and Johnston, A. C., 1992, Common features of the excitation and propagation of strong ground motion for North American earthquakes: Seismological Society of America Bulletin, v. 82, p. 1–23.

Harp, E. L., and Wilson, R. C., 1989, Shaking intensity thresholds for seismically induced landslides: Geological Society of America Abstracts with Programs, v. 21, no. 5, p. 90.

Heaton, T. H., Tajima, F., and Mori, A. W., 1986, Estimating ground motions using recorded accelerograms: Surveys in Geophysics, v. 8, p. 25–83.

Jibson, R. W., 1985, Landslides caused by the 1811–12 New Madrid earthquakes [Ph.D. dissert.]: Stanford, California, Stanford University, 232 p.

Jibson, R. W., and Keefer, D. K., 1984, Earthquake-induced landslides in the central Mississippi Valley, Tennessee and Kentucky, *in* Gori, P. L., and Hays, W. W., eds., Symposium on the New Madrid Seismic Zone, Proceedings: U.S. Geological Survey Open-File Report 84-770, p. 353–390.

Jibson, R. W., and Keefer, D. K., 1988, Landslides triggered by earthquakes in the central Mississippi Valley, Tennessee and Kentucky: U.S. Geological Survey Professional Paper 1336-C, 24 p.

Jibson, R. W., and Keefer, D. K., 1989, Statistical analysis of factors affecting landslide distribution in the New Madrid seismic zone, Tennessee and Kentucky: Engineering Geology, v. 27, p. 509–542.

Keefer, D. K., and Wilson, R. C., 1989, Predicting earthquake-induced landslides, with emphasis on arid and semi-arid environments, *in* Sadler, P. M., and Morton, D. M., eds., Landslides in a semi-arid environment: Riverside, California, Inland Geological Society, v. 2, p. 118–149.

Krinitzsky, E. L., and Marcuson, W. F., III, 1983, Principles for selecting earthquake motions in engineering design: Association of Engineering Geologists Bulletin, v. 20, no. 3, p. 253–265.

Lambe, T. W., and Whitman, R. V., 1969, Soil mechanics: New York, John Wiley and Sons, 553 p.

McGee, W. J., 1891, The Lafayette Formation: U.S. Geological Survey 12th Annual Report, pt. 1, p. 387–521.

McGee, W. J., 1893, A fossil earthquake: Geological Society of America Bulletin, v. 4, p. 411–414.

Newmark, N. M., 1965, Effects of earthquakes on dams and embankments: Geotechnique, v. 15, no. 2, p. 139–160.

Nuttli, O. W., 1973, The Mississippi Valley earthquakes of 1811 and 1812—Intensities, ground motion, and magnitudes: Seismological Society of America Bulletin, v. 63, p. 227–228.

Nuttli, O. W., 1982, Damaging earthquakes of the central Mississippi Valley, *in* McKeown, F. A., and Pakiser, L. C., eds., Investigations of the New Madrid, Missouri, seismic zone: U.S. Geological Survey Professional Paper 1236, p. 15–20.

Nuttli, O. W., 1983, Average seismic source-parameter relations for mid-plate earthquakes: Seismological Society of America Bulletin, v. 73, no. 2, p. 519–535.

Nuttli, O. W., and Herrmann, R. B., 1984, Ground motion of Mississippi Valley earthquakes: Journal of Technical Topics in Civil Engineering, v. 110, no. 1, p. 54–69.

Obermeier, S. F., 1989, The New Madrid earthquakes—An engineering-geologic interpretation of relict liquefaction features: U.S. Geological Survey Professional Paper 1336-B, 114 p.

Penick, J. L., 1981, The New Madrid Earthquakes (revised edition): Columbia, Missouri, University of Missouri Press, 176 p.

Potter, P. E., 1955, The petrology and origin of the Lafayette Gravel; part II, geomorphic history: Journal of Geology, v. 63, no. 2, p. 115–132.

Saucier, R. T., 1977, Effects of the New Madrid earthquake series in the Mississippi alluvial valley: U.S. Army Engineers Waterways Experiment Station Soils and Pavements Laboratory, Miscellaneous Paper S-77-5, 25 p.

Seed, H. B., 1979, Considerations in the earthquake-resistant design of earth and rockfill dams: Geotechnique, v. 29, no. 3, p. 215–263.

Siegel, R. A., 1978, STABL user manual: West Lafayette, Indiana, Purdue University, 104 p.

Somerville, P. G., McLaren, J. P., LeFevre, L. V., Burger, R. W., and Helmberger, D. V., 1987, Comparison of source scaling relations of eastern and western North American earthquakes: Seismological Society of America Bulletin, v. 77, no. 2, p. 322–346.

Varnes, D. J., 1978, Slope movement types and processes, *in* Schuster, R. L., and Krizek, R. J., eds., Landslides—Analysis and control: National Academy of Science, Transportation Research Board, Special Report 176, p. 11–33.

Wieczorek, G. F., Wilson, R. C., and Harp, E. L., 1985, Map showing slope stability during earthquakes of San Mateo County, California: U.S. Geological Survey Miscellaneous Geologic Investigations Map I-1257E, scale 1:62,500.

Wilson, R. C., and Keefer, D. K., 1983, Dynamic analysis of a slope failure from the 6 August 1979 Coyote Lake, California, earthquake: Seismological Society of America Bulletin, v. 73, no. 3, p. 863–877.

Wilson, R. C., and Keefer, D. K., 1985, Predicting areal limits of earthquake-induced landsliding, *in* Ziony, J. I., ed., Evaluating earthquake hazards in the Los Angeles region—An earth-science perspective: U.S. Geological Survey Professional Paper 1360, p. 316–345.